Conference Paper, Published Version

Albayrak, Ismail; Nikora, Vladimir; Miler, Oliver; O'Hare, Matthew

Flow-plant interaction at a leaf scale: effects of leaf shape and flexural rigidity

River Flow 2010 - Dittrich, Koll, Aberle & Geisenhainer (eds) - © 2010 Bundesanstalt für Wasserbau ISBN 978-3-939230-00-7

Flow-Plant Interaction at a Leaf Scale: Effects of Leaf Shape and Flexural Rigidity

I. Albayrak, V. Nikora & O. Miler
School of Engineering, Fraser Noble Building, University of Aberdeen, AB24 3UE Aberdeen, UK

M. O'Hare
Centre for Ecology & Hydrology Edinburgh, Bush Estate, Penicuik, Midlothian, EH26 0QB, UK

ABSTRACT: The effect of leaf shape and flexural rigidity on drag force imposed by flowing water and its time variability are experimentally studied in an open-channel flume at seven leaf Reynolds numbers ranging from 0.5×10^4 to 3.5×10^4. The study involved artificial leaves of the same surface area but with three distinctly different shapes ('rectangular', 'elliptic', and 'pinnate') and with three flexural rigidities. Instantaneous drag forces and flow velocities have been measured using a drag measurement device synchronized with two ADVs. The results revealed that when exposed to a fluid flow, the elliptic leaf has better hydrodynamic shape as it experienced less drag force, with the rectangular leaf showing slightly less efficiency. However, the pinnate leaf experienced higher drag force than the other leaves due to its complex geometry with six leaflets, larger perimeter, width and frontal area. Flow separation from six leaflets of the pinnate leaf prevents leaf reconfiguration such as leaflets folding and/or streamlining. Experiments show that the magnitude of the leaf shape effect on drag force depends on leaf rigidity. A linear relation between the drag force and velocity was found for flexible elliptic and rectangular leaves with low rigidity. For more rigid elliptic and rectangular leaves, the drag force scaled with squared velocity. This suggests that lower rigidity allowed the elliptic and rectangular leaves to undulate and streamline better in the flow in order to reduce the drag forces. However, for the pinnate leaf, no significant effect of rigidity on the relation between the drag force and velocity was found. The Vogel number ranged from -0.41 and -0.34 and the drag coefficient decreased with increase in Reynolds number for all rigidities for the pinnate leaf. The results indicate that leaf geometry and flexural rigidity play an important role in the leaf reconfiguration and thus in the adaptation of aquatic plants to flow conditions.

Keywords: Aquatic plants, Leaves, Drag force, Drag coefficient, Reconfiguration, Flexural rigidity, River flow

1 INTRODUCTION

Aquatic plants encounter drag forces imposed by flowing water at multiple scales such as patch, plant, stem and leaf scales. In general, plants may minimize drag forces by minimizing their surface area or/and streamlining in the flow direction. Although the role of individual plant leaves in drag reduction and control is important, very little is known about the physical mechanisms involved. To resist successfully high flow loads without damage, plants develop different strategies such as the shape reconfiguration of the leaves and the bending of the stems into the canopy. These help plants to streamline and reduce the surface and projected area exposed to the flow that results in a reduction of the drag force and drag coefficient with increasing flow velocity leading to the enhancement of plant performance (Usherwood et al. 1997, Sand-Jensen 2003, Nikora 2009).

Compared to terrestrial plants, aquatic plants are much less studied with respect to drag control. There is practically no information available in relation to flow-plant interactions at the leaf scale. Vogel (1989) investigated the drag acting on broad leaves of a variety of terrestrial species and reported that broad-leaved species reconfigured their leaf shapes into cones to reduce the drag force exerted by wind. Schouveiler et al. (2006) investigated the mechanism of reconfiguration of broad leaves subjected to wind force and derived a scaling law from the mechanical equilibrium for a circular plastic sheet. Langre (2008) reviewed the effect of wind on plants in relation to the mechanical interactions between wind and plants, from plant organs to plant systems. In relation to

aquatic plants, Sand-Jensen (2003) investigated drag and reconfiguration of freshwater macrophytes and found that increasing flexibility leads to greater reconfiguration and lower drag coefficients. Flexible plants experience a steeper decline of drag coefficients with increasing water velocity compared to rigid plants, i.e., flexible plants mounted vertically on a horizontal substratum bend over in fast flow attaining a shielded near-bed position of low drag. This shows the importance of bio-mechanical properties such as bending and tensile properties of plants and leaves in the reduction of drag force.

The hydrodynamic effects of shape and size change during reconfiguration of a flexible macroalga were studied by Boller et al. (2006). In this study, whole-plant realignment at low velocities and compaction of the crown reducing the frontal area at higher velocities were found as two separate mechanisms of reconfiguration. In hydraulic engineering, aquatic plants are considered as roughness creating resistance to flow and thus many experimental studies of vegetation resistance in open channel flows have been completed (Kouwen and Fathi-Moghadam 1997, 2000; Armanini et al. 2005).

The flow-induced drag force F is typically parameterized as:

$$F = 1/2\rho A C_D U^2 \tag{1}$$

where U is flow velocity, ρ is fluid density, A is a representative area, and C_d is the drag coefficient. Application of (1) for aquatic plants and leaves is not straightforward because they are flexible and tend to reduce the drag force by changing their forms and representative area via bending and folding. For instance, the deviation from the velocity-squared relationship may be associated with reconfiguration rather than with a change in the Reynolds number Re. Vogel (1989, 1994) expressed this in terms of an exponent v (known today as the Vogel number), so the drag force scales with velocity as U^{2+v}. If a leaf is rigid and Re is very high (so we can assume that $C_D = const$), its drag force is a function of U^2 (i.e., $v = 0$). For a flexible leaf, $v < 0$ and in many cases one may observe $v \approx -1$ because of leaf reconfiguration (Vogel, 1989).

The objective of this study is to investigate experimentally the effect of leaf shape and flexural rigidity on the drag force and its time variability in relation to reconfiguration and associated drag control/reduction. In order to achieve this objective, a series of experiments with artificial leaves of different shapes and rigidities has been completed in the Fluid Mechanics Laboratory of the University of Aberdeen. Below we first outline our experimental set up, then present experimental results and their discussion in connection to plant performance in flows.

2 EXPERIMENTAL SET-UP

All experiments were carried out in a glass sided tilting flume with a flat bed. The flume is B =0.3 m wide, L=12.5 m long and H=0.45 m deep (Figure1). Seven different flow rates with the constant water depth h=0.15 m and bed slope 1:1000 were studied (Table 1). Since the depth and the bed slope were fixed, the hydraulic conditions deviated from the uniform flow regime. This deviation, however, was not critical for our study that focused on the local phenomenon of flow-leaf interactions. Measurements were carried out at a location 7 cm from the bed within the flume section 5 to 6 m from the flume entrance, where the flow field was fully developed with nearly homogeneous vertical profile of the longitudinal velocity. A standard experiment involved synchronous measurements of instantaneous drag force and flow velocities (with two ADVs, one in front of a leaf and another in the leaf wake), which have been supplemented with leaf video recordings. A range of three shapes and three rigidities of specially manufactured artificial leaves have been studied. Table 1 presents the hydraulic parameters for the experiments performed for each leaf type (see definitions and explanations in the following subsections). In Table 1, the 'leaf' Reynolds number (Re) and 'depth' Reynolds number (Re_h) are computed as follows:

$$\mathrm{Re} = U_a \sqrt{S} / \upsilon \tag{2}$$

$$\mathrm{Re}_h = U_d h / \upsilon \tag{3}$$

where U_a, U_d are leaf approaching and depth-averaged velocities, respectively, S is the surface area of a leaf (equal to 0.0016 m^2), h is the water depth and υ is the kinematic viscosity.

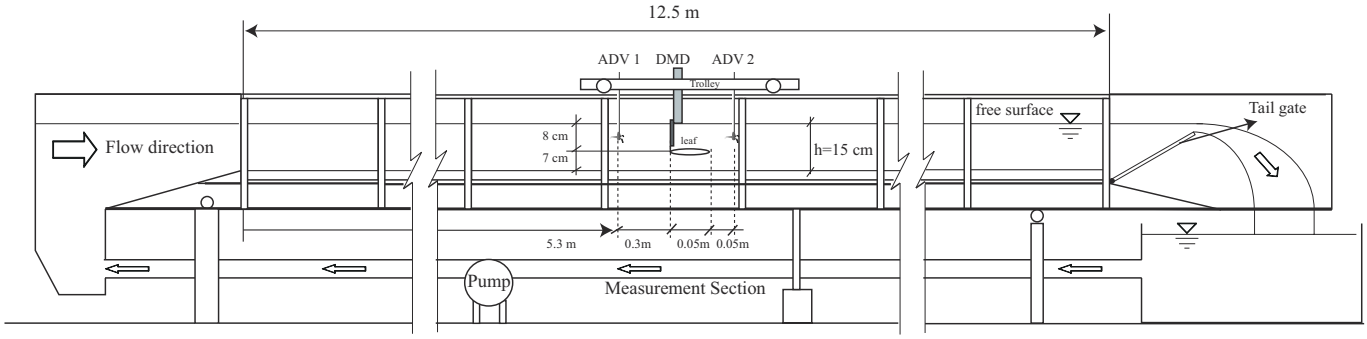

Figure 1. Schematic diagram of a glass sided tilting flume set-up, measurement section, and position of ADVs and DMD.

Table 1. Hydraulic parameters for the experiments.

h m	Q m^3/s	U_d m/s	Re	Re_h
0.15	0.009	0.20	8.02×10^3	30.07×10^3
0.15	0.014	0.30	12.09×10^3	45.33×10^3
0.15	0.018	0.40	16.00×10^3	60.00×10^3
0.15	0.022	0.50	19.90×10^3	74.63×10^3
0.15	0.027	0.60	23.91×10^3	89.66×10^3
0.15	0.032	0.70	28.09×10^3	105.33×10^3
0.15	0.036	0.80	31.87×10^3	119.51×10^3

2.1 *Measurement Devices*

2.1.1 *Acoustic Doppler Velocimeter (ADV)*

Velocity measurements were carried out by two Acoustic Doppler Velocimeters (ADV) at 7 cm above the flume bed (Figs. 1 and 2). The up-stream ADV was placed 30 cm away from the submerged tube of the Drag Measurement Device (DMD, Figure 2) in order to measure the approach velocity and turbulence characteristics of the flow without any effect of a leaf. The downstream ADV was placed 5 cm way from the back tip of a leaf to measure velocity and turbulence characteristics in the wake region of a leaf (Figure 1). Two ADVs were synchronized with DMD by an in-house electronic circuit. The ADVs and DMD were set to work at a sampling rate of 50 Hz for 5 minutes, as a standard set-up for each experimental scenario. The coordinate system is defined in Figure 2b.

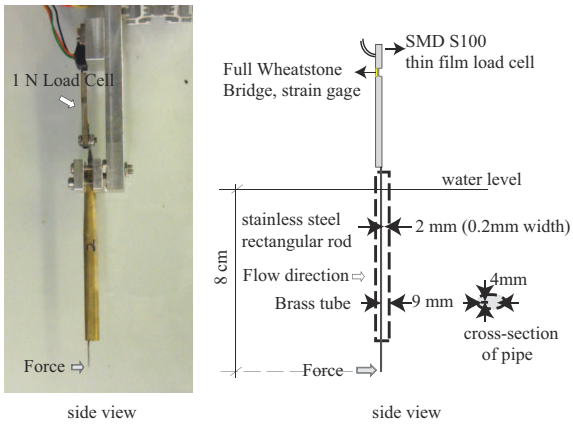

a) Drag Measurement Device (DMD)

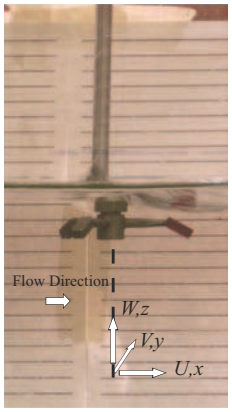

b) Acoustic Doppler Velocimeter (ADV).

Figure 2. (a) Drag Measurement Device (DMD), (b) Acoustic Doppler Velocimeter (ADV).

2.1.2 *Drag Measurement Device (DMD)*

The DMD for this study has been specially developed by the authors to measure drag force on a leaf and/or shoot (Figure 2a). The design of the DMD is based on a small range load cell with an extended beam allowing to measure micro scale drag forces (mN) with high accuracy and temporal resolution. The DMD works at sampling frequency from 1 Hz to 1000 Hz and measures mNewton range forces. The DMD shown in Figure 2a consists of a load cell, an elliptic shaped brass tube and a 10 cm high, 2 mm wide and 0.2 mm thick stainless steel rod. The rod is attached to the load cell as an extension of the beam and

placed vertically in the center of the brass tube. A leaf can be easily attached to the tip of the rod by using super-glue. Any force applied to the rod and an associated leaf along the flow direction (Figure 2a) results in deflection of the rod and the beam, leading to deflection of full wheatstone bridge and generation of a voltage signal. The measured drag force on the tip without a leaf did not exceed 10% of the total measured drag (i.e., tip + leaf), being around 2.5-5% in most cases. The DMD data analysis involved subtraction of the rod contribution from the total measured drag so that only drag force acting on the leaves was used in the interpretations.

2.1.3 *Video Recording*

For visualization of flow-leaf interaction, a half megapixel DV camera with sampling rate of 25 Hz was used in all experiments and 5 minutes video recording were made synchronously with drag force and velocity measurements. A 40 cm by 30 cm area was covered and recorded by the camera.

2.2 *Experimental Leaves*

To simulate basic geometries of a leaf in our experiments, elliptic, pinnate and rectangular geometric shapes were chosen (Figure 3). The leaf surface area of each shape was kept constant and was equal to 0.0016 m^2. Elliptic, pinnate and rectangular shapes were coded as S1, S2 and S3, respectively. In order to examine the effect of rigidity of a leaf on drag force, leaves were made of plastic materials with different values of Young modulus and thickness. The mechanical properties of simulated leaves (Young's modulus, flexural rigidity, and second moment of area) are shown in Table 2. The details of tension and bending tests of the materials can be found in Miler et al. (2010). Based on the flexural rigidities of the experimental leaves, flexible, moderate rigid and highly rigid leaves were coded as R1, R3, and R5, respectively.

Table 2. Properties of the plastic leaves used in the experiments.

Exp. Code	Second moment of area I, m^4	Young modulus (Tension) E, Nm^{-2}	Flexural rigidity IE, Nm2
R1	6.25×10^{-17}	60×10^{8}	0.375×10^{-6}
R3	6.65×10^{-16}	58.8×10^{8}	3.9×10^{-6}
R5	6.63×10^{-14}	12.5×10^{8}	83.2×10^{-6}

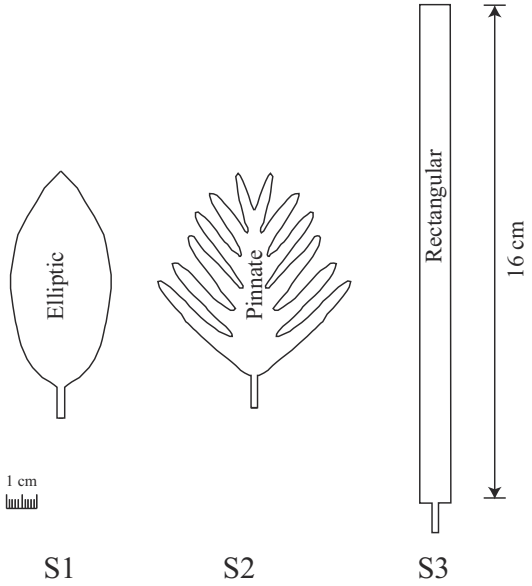

Figure 3. Leaf shapes.

2.3 *Experimental Procedure*

For each of 9 leaf types (Table 3), velocity and drag force measurements and video recordings were carried out with synchronized ADVs, DMD and DV camera for 5 minutes at 7 different flow rates (Table 1). First, a leaf was glued to the tip of the steel rod of the DMD and then a zero-call of the DMD was made in a fishing tank where leaf was 8 cm below the water surface. Vishay model 6000 scanner was used for data recording. Second, the DMD was positioned in the center of the flume between two ADVs as shown in Figure 1. The centers of the leaf and the ADVs' sampling volumes were on the same horizontal axis positioned at 7 cm above the flume bed and at 8 cm below the water surface. The data collected from the ADVs, DMD and video camera were transferred to a high-speed computer for the post-processing and data analysis. The drag coefficient (C_d) was calculated by using the following equation:

$$C_d = 2F/(\rho A_w U_a^2) \tag{4}$$

where F is the drag force, ρ is the density of water, A_w is the leaf wetted area (0.0032 m^2) and U_a is the leaf approaching velocity.

In this paper, we focused on the effects of leaf shape and rigidity on the mean drag force and the drag coefficient at different flow velocities. The shape and rigidity effect on drag and velocity statistics and the image analysis will be reported in the follow up study.

Table 3. Experimental matrix and codes of experiments.

Rigidity	R1		
Shape	S1	S2	S3
Code	R1S1	R1S2	R1S3
Rigidity	R3		
Shape	S1	S2	S3
Code	R3S1	R3S2	R3S3
Rigidity	R5		
Shape	S1	S2	S3
Code	R5S1	R5S2	R5S3

3 EXPERIMENTAL RESULTS AND DISCUSSION

3.1 *Effect of leaf shape on drag force and drag coefficient*

In Figure 4, the time-averaged drag forces of elliptic, pinnate and rectangular shape leaves at three different flexural rigidities (R1, R3 and R5) are shown as a function of mean upstream velocity. There are large differences in the drag force experienced by the pinnate leaf and the other two leaf shapes for all three rigidities. The drag force on the pinnate leaf is the largest at all velocities and significantly diverging from the drag force on the other two leaves as velocity increases, irrespective of leaf rigidity.

In Figure 4a, at lower velocities the drag on the rectangular leaf is slightly lower than the drag on the elliptic leaf, but with increase in velocity this trend changes to opposite. At medium rigidity (R3), the elliptic leaf has the lowest drag at all velocities, with the rectangular leaf having slightly higher drag. This situation changes with increase in rigidity (Figure 4c), i.e., the drag forces on the elliptic and rectangular leaves are almost the same for the velocity less than 0.6 m/s, with only a small difference at higher velocity. On average, the drag forces on the pinnate leaf are 75%, 65% and 105% more than on the elliptic leaf, and 70%, 30% and 90 % more than on the rectangular leaf at the lowest, moderate and highest rigidities, respectively. This result indicates that the effect of leaf shape on drag force is strong and may be significantly enhanced by leaf serration. Indeed, it is most likely that the pinnate leaf experiences the highest drag force because of its complex geometry with six leaflets, and larger perimeter, width, and frontal area. Flow separations from six leaflets of the pinnate leaf enhance instabilities that prevent reconfiguration in the form of folding and streamlining of its leaflets.

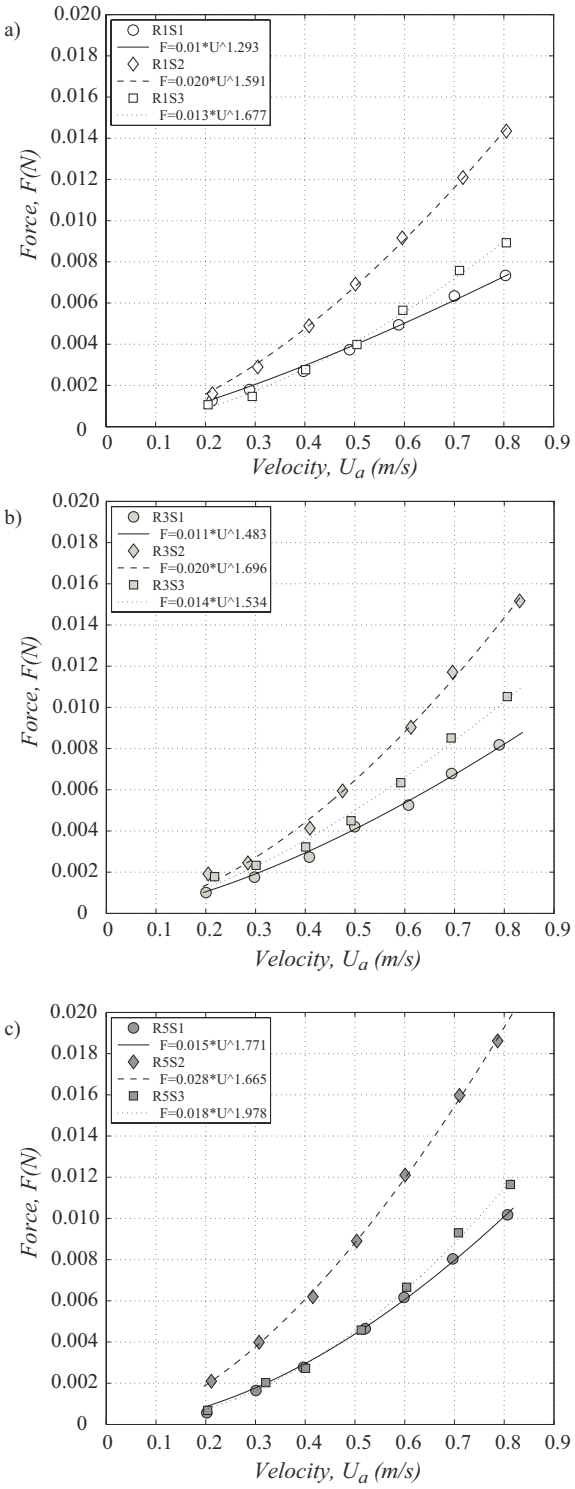

Figure 4. Drag force F of elliptic, pinnate and rectangular leaves as a function of mean upstream velocity for flexural rigidities R1 (a), R3 (b), and R5 (c).

The drag coefficients $C_d=f(Re)$ for the different leaf shapes at three different rigidities are shown in Figure 5. For the rigidity R1, a considerable decrease of the drag coefficient with increasing Re for all leaf shapes is noticeable. Also, the drag coefficient of the pinnate leaf is approximately 60-70% higher than the drag coefficients of the elliptic and rectangular leaves, respectively. The drag coefficient of the rectangular leaf at small Re is slightly lower than that for the elliptic leaf whereas it is slightly higher at larger Re (Figure 5a). For the medium rigidity,

R3, the curves $C_d=f(Re)$ for different leaf shapes are separated within the whole range of Re, with the highest C_d for the pinnate leaf and the lowest C_d for the elliptic leaf, as one would expect. (Figure 5b).

With further increase in rigidity (Figure 5c), the shape of $C_d=f(Re)$ curve for the pinnate leaf remains similar to that for lower rigidities although C_d values become much higher. The drag coefficients of the rectangular and elliptic leaves nearly coincide and are approximately constant, being 50-250% less than C_d for the pinnate leaf. The results clearly show that, overall, the elliptic leaf has the best hydrodynamic shape among the leaves as it experiences the least drag force, with the rectangular leaf performing slightly worse but still much better that the pinnate leaf.

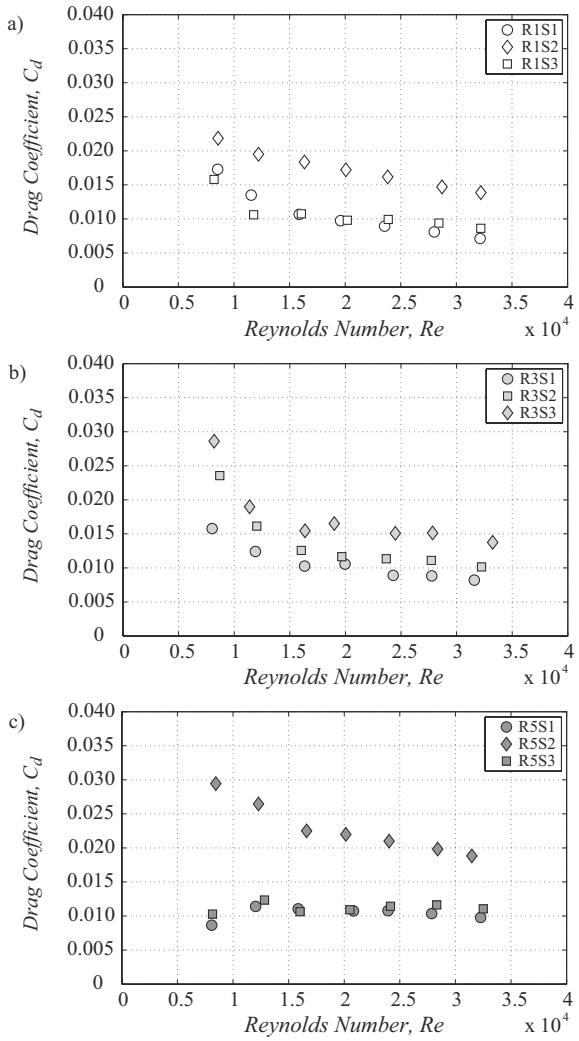

Figure 5. Effect of leaf shape and rigidity on drag coefficient for a range of Re (R1a, R3b, and R5c).

3.2 *Effect of flexural rigidity on drag force and drag coefficient*

In this section, we consider the effect of the flexural rigidity on drag force and drag coefficient for each leaf shape separately. Figure 6a shows the drag force on the elliptic leaf as a function of mean upstream velocity for the rigidities R1, R3 and R5. The drag force increases with the velocity, as expected, but the effect of rigidity becomes visible only at velocities higher than 0.5 m/s. For this range of higher velocities, drag force increases with increase in rigidity. A similar effect is also seen in Figure 6b showing dependence of the drag coefficient on Re. Such a behavior suggests that decrease in rigidity leads to a higher capability of a leaf for re-configuring and fluttering leading to a drag reduction.

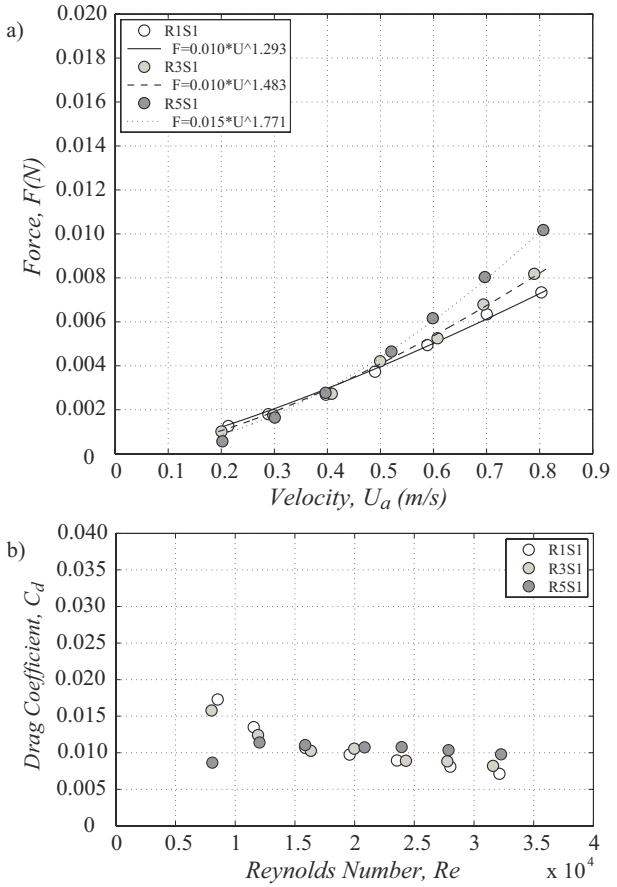

Figure 6. (a) Plot of the drag force versus the mean upstream velocity; and (b) the drag coefficient versus Reynolds number for the elliptic leaf with three different rigidities.

Figure 7 shows the drag force-velocity and drag coefficient-Reynolds number relations for the pinnate leaf. For the rigidities R1 and R3, the drag forces on the leaves have similar tendency and magnitude, whereas for the highest rigidity R5 the pinnate leaf is exposed to much higher drag force, with significantly higher drag coefficients.

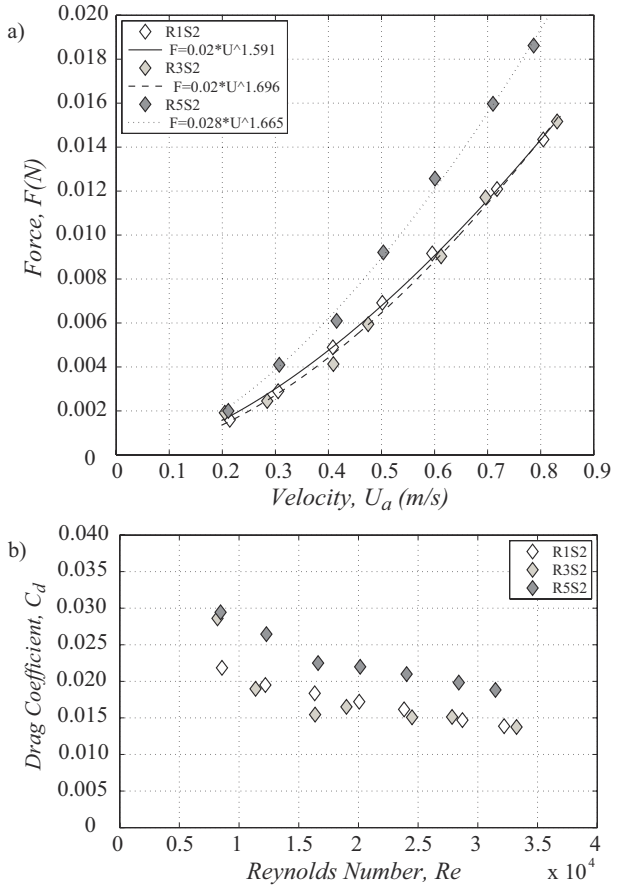

Figure 7. (a) Plot of the drag force versus the mean upstream velocity and (b) the drag coefficient versus Reynolds number for the pinnate leaf with three different rigidities.

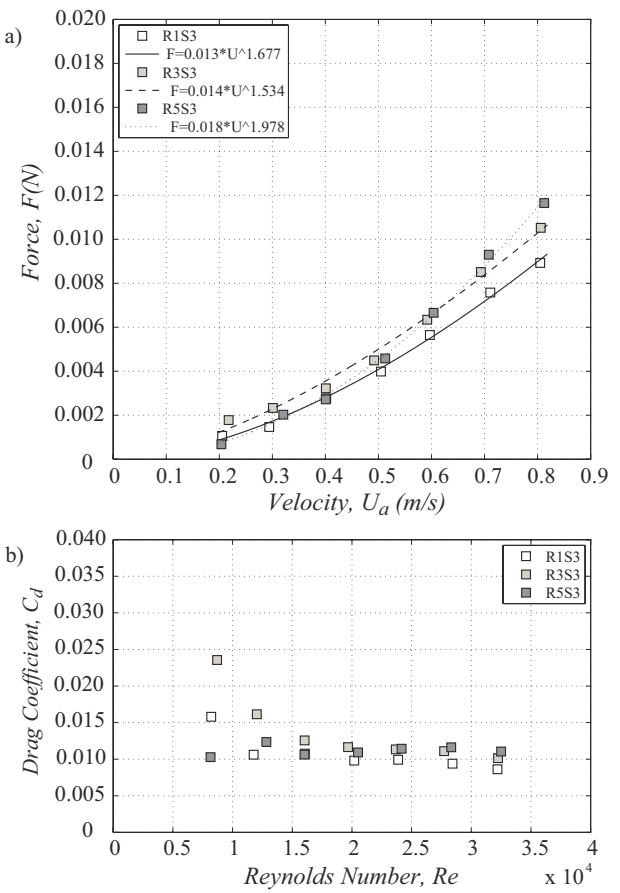

Figure 8. (a) Plot of the drag force versus the mean upstream velocity and (b) the drag coefficient versus Reynolds number for the rectangular leaf with three different rigidities.

With regard to Figure 8, the drag force on the most rigid rectangular leaf is the highest, followed by the moderate and low rigidity leaves. This difference becomes more significant with increasing velocity. Also, the effect of rigidity on the drag coefficient is most profound at low Re, becoming negligible at high Re.

The artificial leafs we used in this study were similar in shape and flexural rigidity to natural leaves. The pinnate, rectangular and elliptic leaves broadly resemble the leaves of aquatic plant species, e.g. *Myriophyllum alterniflorum* (pinnate shape), *Glyceria fluitans* (rectangular shape) and *Elodea canadensis* (elliptic shape). The flexural rigidity of *G. fluitans* leaves is the same order of magnitude of the most flexible leaves in our study (Miler and Albayrak, unpublished data). Hence, we can conclude that the drag reduction through leaf reconfiguration in natural strap-like leaves of *G. fluitans* will be similar or better than in the artificial rectangular leaf with rigidity R1 in our study. However, in addition to shape and rigidity, also other leaf properties like serration, thickness and roughness influence the reconfiguration and drag reduction of the leaves. Therefore, the further investigation on these properties of leaves is needed in order to better understand flow-plant interactions at the leaf scale.

4 CONCLUSION

Extensive and systematic experimental measurements of drag force and velocity were conducted in an open-channel flow for three leaf geometries (elliptic, pinnate and rectangular) covering three flexural rigidities ranging from low to high.

When exposed to the load of a fluid flow, the pinnate leaf experienced higher drag force and drag coefficient than the other leaves due to its complex geometry with six leaflets, larger perimeter, width, and frontal area. Flow separation from six leaflets of the pinnate leaf creates a variety of instabilities preventing reconfiguration of the pinnate leaf such as folding and streamlining in order to reduce the drag imposed by flow. On the other hand, the elliptic leaf has a better hydrodynamic shape than the other leaves as it experiences less drag force due to a streamlined shape and smaller frontal area. The rectangular leaf presented a behavior similar to the elliptic leaf.

The effect of flexural rigidity on drag force and drag coefficient for each leaf shape was examined. For the elliptic and rectangular leaves with lower rigidity, it was found that the drag forces on the leaves were lower and scaled quasi-linearly with the velocity similar to a flexible body in the flow (Vogel 1994). Low rigidity allowed the elliptic and rectangular leaves to undulate and streamline in the flow that reduced the drag. For the highest rigidity, the elliptic and rectangular leaves experienced higher drag forces than those with lower rigidity. For this case, the drag force was a function of squared velocity while the drag coefficients were quasi-constant (i.e., largely independent on Re). However, for the pinnate leaf, the drag coefficient was decreasing as Reynolds number was increasing for all rigidities. The most rigid pinnate leaf experienced the highest drag forces at all flow rates, while the pinnate leaves with moderate and low rigidities showed much lower drag forces.

To summarize, our results yield a first step towards the understanding of plant-flow interactions at the leaf scale and indicate that geometry and flexural rigidity strongly affect leaf performance, i.e., their potential capabilities for adaptation to different habitats. The focus of the follow up study will be on the shape and rigidity effects on drag and velocity statistics.

ACKNOWLEDGEMENTS

The work was partly supported by the Leverhulme Trust, Grant F/00152/Z 'Biophysics of flow-plant interactions in aquatic systems'. The authors are grateful to Giulia Pagello for her help with the experimental work.

REFERENCES

Armanini, A., Righetti, M., Grisenti, P. 2005. Direct measurement of vegetation resistance in prototype scale. J. Hydraul. Res., 43, 481–487.

Boller, M. L., Carrington, E. 2006. The hydrodynamic effects of shape and size change during reconfiguration of a flexible macroalga. J. Exp. Biol., 209, 1894-1903.

Langre E. 2008. Effects of wind on plants. Annual Review of Fluid Mechanics, 40, 141-168.

Kouwen, N., Fathi-Moghadam, M. 1997. Nonrigid, nonsubmerged, vegetative roughness on floodplains. J. Hydraul. Eng. ASCE, 123(1), 51–57.

Kouwen, N., Fathi-Moghadam, M. 2000. Friction factors for coniferous trees along rivers. Hydraul.Eng. ASCE ,126(10), 732–740.

Miler, O., Albayrak, I., Nikora, V., O'Hare, M., Crane, T. 2010. Biomechanics of aquatic plants and its role in flow-vegetation interactions. Conference paper, River-Flow, Braunschweig, Germany.

Nikora, V. 2009. Hydrodynamics of aquatic ecosystems: an interface between ecology, biomechanics and environmental fluid mechanics. River Research and Applications, DOI: 10.1002/rra.1291.

Sand-Jensen K. 2003. Drag and reconfiguration of freshwater macrophytes. Freshwater Biology, 48, 271–283.

Schouveiler L., Boudaoud A. 2006. The rolling up of sheets in a steady flow. J. Fluid Mech., 563, 71-80,

Usherwood J. R., Ennos A. R., Ball D.J. 1997. Mechanical adaptations in terrestrial and aquatic buttercups to their respective environments. Journal of Experimental Botany, 48, 1469–1475.

Vogel, S. 1989. Drag and reconfiguration of broad leaves in high winds. J.Exp. Bot. 40, 941-948.

Vogel, S. 1994. Life in Moving Fluids (2nd edn). Princeton: Princeton University Press.